DC SQUIDS 1980: THE STATE OF THE ART

M. B. Ketchen
IBM Thomas J. Watson Research Center
Yorktown Heights, New York 10598

The four primary areas of concern in the development of high performance dc SQUIDs are white noise, 1/f noise, readout schemes, and coupling. For an optimized dc SQUID the intrinsic energy sensitivity in the white noise region is given by $\varepsilon_w = \gamma_1 hk_B T(eI_oR)^{-1} + \gamma_2 h$, where I_o is the critical current per junction and R is the shunt resistance per junction. γ_1, which multiplies the thermal noise contribution, and γ_2, which multiplies the shot noise/zero point fluctuation contribution, are numerical factors of order unity. Values of ε_w approaching h have recently been measured for several members of a new generation of low noise dc SQUIDs. The intrinsic energy sensitivity in the 1/f noise region, ε_f, is predicted to scale as $(I_oR)^2$ for tunnel junctions. This may impose significant low frequency limitations on SQUIDs with very low values of ε_w. Readout schemes for high sensitivity dc SQUIDs will require further development. At the moment primarily small signal amplifier readout schemes are being used to evaluate the new generation of low noise SQUIDs. Planar thin-film coupling schemes are about to have a big impact on dc SQUID design. Such schemes can achieve tight coupling between SQUID and input coil, and can be implemented using the same fabrication techniques that produce SQUIDs with low values of ε_w.

Introduction

This paper first reviews the familiar characterization of the dc SQUID (Superconducting QUantum Interference Device). White and 1/f noise are then discussed with particular emphasis placed on the role of the I_oR product in determining SQUID performance. Readout schemes presently in use are described. A brief review of the performance of some of the members of the new generation of low noise dc SQUIDs is given. An example illustrating the principles of an efficient planar coupling scheme is discussed in detail, and some rather simple but general results are given that should apply to a wide range of tightly coupled SQUID designs.

Characterization of the dc SQUID

The dc SQUID[1] consists of two Josephson elements[2] in a superconducting loop of inductance L (Fig. 1). The Josephson elements are typically Josephson tunnel junctions which are well represented by the resistively shunted junction model.[3,4] Each junction has a critical current I_o and is shunted by a linear resistance R and a capacitance C. Magnetic flux can be coupled to the SQUID either by application of an external magnetic field or by passing a current through an input coil of inductance L_i situated in close proximity to the SQUID. The maximum zero-voltage current I_m that can be passed through the SQUID in the absence of an applied magnetic flux is $2I_o$. If magnetic flux is applied to the SQUID in a linearly increasing fashion, I_m will decrease, reach a minimum, and then return back to its original value. Further increases in the applied flux will result in repeated oscillations in I_m exhibiting a period of ϕ_o, where $\phi_o = h/2e$ is the flux quantum. The current voltage characteristic of a symmetric SQUID with an integral or half integral number of flux quanta applied is shown in Fig. 2. As the applied flux ϕ is varied, the current-voltage characteristic oscillates between these two extreme cases. The critical current modulation depth $\Delta I_m/2I_o$ is a function of the parameter β[5,6], where

$$\beta = 2LI_o/\phi_o. \tag{1}$$

$\Delta I_m/2I_o$ is about 50% if $\beta = 1$. For any value of applied flux the current-voltage characteristic is single valued provided the hysteresis parameter β_c[3,4] is less than unity, where

$$\beta_c = \frac{2\pi I_o R^2 C}{\phi_o}. \tag{2}$$

It will be shown that the characteristic voltage I_oR is an extremely important parameter in characterizing the performance of the SQUID.

If the flux applied to the SQUID is varied while the bias current I is maintained at some constant value I_B, the voltage V across the SQUID will oscillate with a period of ϕ_o. The shape of $V(\phi)$ will depend on the value of I_B. Representative $V(\phi)$ curves corresponding to the current-voltage characteristics of Fig. 2 are shown in Fig. 3. If $I_B << I_o$ most of the period will be spent in the zero-voltage state with a small region of non-zero voltage near $0.5\phi_o$. As I_B is increased, more and more of the period is spent in the non-zero voltage state until finally, when $I_B \approx 2I_o$, the SQUID is continuously in the $V > 0$ state. As I_B is further increased the amplitude of the voltage modulation decreases, eventually becoming zero for $I_B >> 2I_o$.

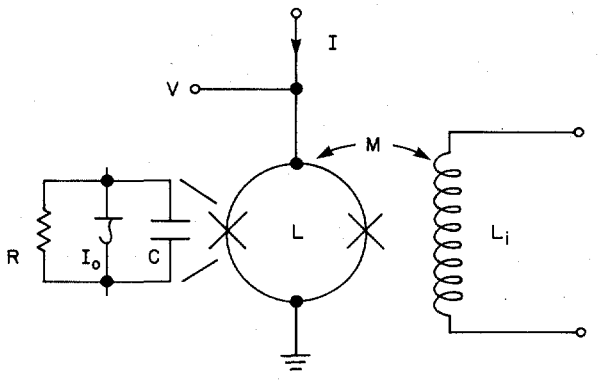

Fig. 1 dc SQUID consisting of two resistively shunted tunnel junctions in a superconducting loop of inductance L. A current through the input coil L_i couples a magnetic flux into the SQUID via the mutual inductance M.

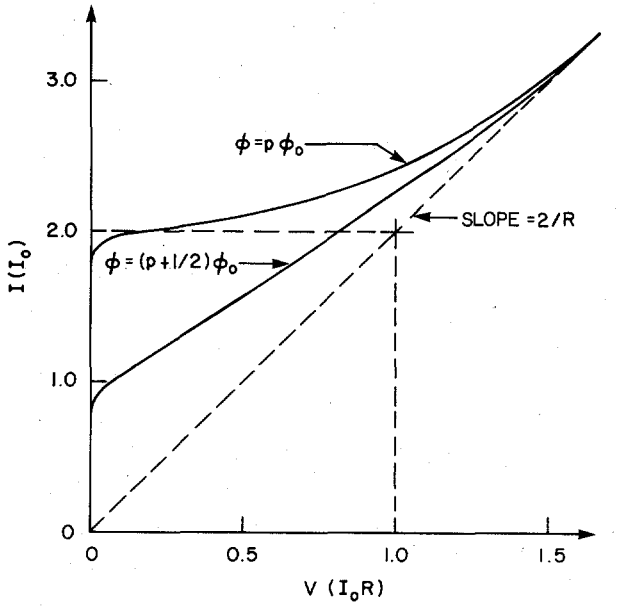

Fig. 2 Current-voltage characteristics of a symmetric SQUID with the applied flux equal to integral (p) and half integral multiples of ϕ_o.

0018-9464/81/0100-0387$00.75 © 1981 IEEE

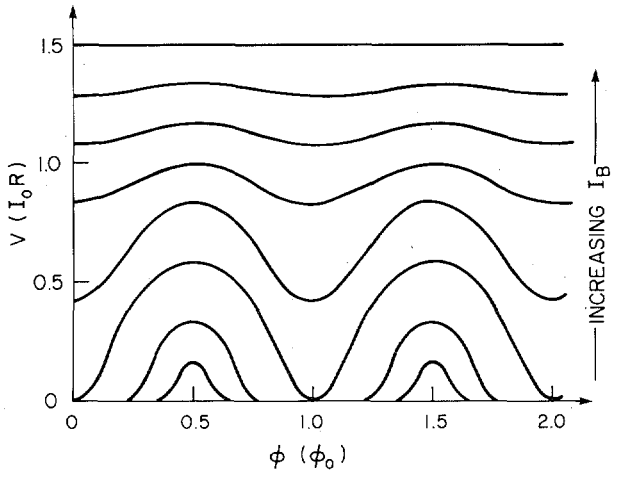

Fig. 3 Voltage versus flux characteristics of a symmetric SQUID for different values of the bias current I_B.

Although there are some situations where one uses a bare SQUID to measure flux changes, it is generally the case that the signal to be measured is converted into a current which is passed through an input coil (Fig. 1). This current then generates a flux which is coupled to L via a mutual inductance M. Let I_s be the current in the input coil in a 1 Hz bandwidth that can be detected by the SQUID with a signal-to-noise ratio of unity. Let ϕ_n be the equivalent SQUID flux noise in the 1 Hz bandwidth so that $MI_s = \phi_n$. The minimum energy in the 1 Hz bandwidth that can be detected in the input coil is then $L_i I_m^2/2$ or $\phi_n^2/2k^2L$ where $k^2 = M^2/L_iL$. This energy depends on the noise characteristics of the SQUID and upon k^2. It is a useful quantity for comparing different SQUIDs.[7,8] Generalizing to all frequencies one can then write a figure of merit ε^c as

$$\varepsilon^c = S_\phi/2k^2L = \varepsilon/k^2, \tag{3}$$

where S_ϕ is the power spectrum of the flux noise in the SQUID and ε is the "intrinsic energy sensitivity" of the SQUID. For certain special cases where a narrow bandwidth can be tolerated, a tuned input circuit can be used to enhance sensitivity.[9] In such situations poor coupling can be compensated for and ε becomes the relevant figure of merit. However, most applications of SQUIDs involve an untuned input circuit, and ε^c is the appropriate figure of merit.

The value of S_ϕ depends strongly on the conditions of flux and current bias as well as the nature of the circuit attached to the input coil.[10] In practice one evaluates S_ϕ by measuring the voltage noise power spectrum S_V across the SQUID at some particular value of I_B and ϕ with a high impedance attached across the input coil. The value of $\partial V/\partial\phi$ is measured at the same point and S_ϕ is calculated from:

$$S_\phi = S_V/(\partial V/\partial\phi)^2. \tag{4}$$

It is generally the case that low values of S_ϕ are associated with maxima in $\partial V/\partial\phi$. For a SQUID with an opened input coil S_ϕ can be attributed to two different sources. One of these is the direct voltage noise across the parallel junctions. The other is a voltage noise arising from a circulating current noise which is at least partially correlated with the direct voltage noise.[11] The existence of the circulating current noise and the degree of correlation between it and the direct voltage noise remain to be verified and measured experimentally. The strong theoretical evidence for this circulating current noise suggests that it should be taken seriously. Such a noise source can couple a noise current into the input circuit. This will then be sensed by the SQUID to produce an additional contribution to S_V of the SQUID. For most practical circuits that one would attach to an input coil the increase in S_V will probably be less than a factor of 2, although there may be special cases where the effect is larger.

Noise tends to round off the sharp corners in the SQUID's characteristic curves[12-16] as shown in Figs. 2 and 3. In the absence of any noise the current-voltage characteristic would intersect the current axis with zero slope. The corresponding $V(\phi)$ curves would exhibit regions of infinite $\partial V/\partial\phi$ near $V=0$ for $I_B < 2I_o$. Noise rounding can be characterized in terms of the noise parameter Γ where

$$\Gamma = \frac{2\pi k_B T}{I_o\phi_o}. \tag{5}$$

The larger Γ is, the more noise rounded the characteristics will be and the smaller will be the maximum value of $\partial V/\partial\phi$. Tesche and Clarke[10] find that with $\Gamma = 0.05$ the maximum $\partial V/\partial\phi$ and best SQUID performance is found with $I_B \approx 1.3(2I_o)$, a prediction that agrees well with experiment.[17] On some of the more recent ultra-low-noise SQUIDs, on the other hand, $\Gamma \approx 0.002$, and the maximum values of $\partial V/\partial\phi$ occur with $I_B < 2I_o$.[18] Experimentally, as well as theoretically in the cases that have been examined, optimum noise performance is found in regions of relative or absolute maxima in $\partial V/\partial\phi$. S_V is also found to be a maximum in such regions, but the effect of a large $\partial V/\partial\phi$ dominates.

The characteristic curves of any real SQUID may also show features exhibiting large values of $\partial V/\partial\phi$ that can be attributed to LC resonances in the SQUID structure itself and/or associated lead structure. While considerable work has been done to enable one to predict SQUID resonances and understand their influence on I-V characteristics,[19-22] it is probably fair to say that much still remains to be done. This is particularly true as regards noise performance in the vicinity of resonance features. Although recent ultra-low-noise SQUIDs have shown optimum noise performance in regions that do not appear to be strongly influenced by resonances, it may be possible to take advantage of resonant features to improve SQUID noise performance.

Noise in SQUIDs

The theory of thermal noise in tunnel junctions and particularly in the dc SQUID has been developed extensively by Tesche and Clarke[10]. Recent work by Voss on single junctions has added considerable insight into the role of capacitance in junction noise.[16] From a practical standpoint a simple approximate theory arising from the work of Tesche and Clarke has been and continues to be a powerful and fairly accurate tool for SQUID design. This theory will be reviewed here briefly and cast into a somewhat different form which demonstrates the significance and utility of the I_oR product.

Detailed numerical calculations have shown that optimum SQUID performance is achieved with $\beta = 2LI_o/\phi_o \approx 1$. The periodic modulation of the SQUID's critical current, ΔI_m, in response to an applied magnetic flux is then about $\phi_o/2L \approx I_o$. The maximum corresponding voltage modulation with the SQUID biased at some constant bias current will be

$$\Delta V \approx \Delta I_m(R/2) \approx \frac{I_oR}{2}. \tag{6}$$

Assuming a roughly triangular V versus ϕ characteristic this leads to a flux-voltage transfer function of

$$\frac{\partial V}{\partial\phi} \approx \frac{\Delta V}{\phi_o/2} \approx R/2L. \tag{7}$$

Provided β_c (Eq. 2) has any value less than approximately unity, the thermal voltage noise across the SQUID is on the order of the Johnson voltage noise of the two shunt resistors in parallel and has a spectral density

$$S_v = 4k_BT(R/2). \tag{8}$$

This leads to a thermal flux noise in the SQUID having spectral density

$$S_\phi = S_v(\partial V/\partial\phi)^{-2} \approx 8k_BTL^2/R. \tag{9}$$

The contribution from any independent circulating current noise is neglected for simplicity.[11] The white intrinsic energy sensitivity

due to the thermal noise is given by

$$\varepsilon_w = \frac{S_\phi}{2L} = \gamma_1 \frac{4k_BT}{R/L} = \gamma_1 h \left(\frac{k_BT}{eI_oR}\right) \qquad (10)$$

where the fact that $2LI_o = \phi_o = h/2e$ has been used. Numerical calculations as well as experimental data show Eq. 10 with $\gamma_1 \approx$ 2-5 to be approximately valid in the thermal noise limit when the noise rounding factor $\Gamma \approx 0.05$. For significantly lower values of Γ the above is assumed to be true in the thermal limit although a detailed theory is lacking at present.

Equation 10 suggests that if k_BT/eI_oR is made arbitrarily small, ε_w will become arbitrarily small. This is of course not the case, and another term must be added. This constant term to be added to Eq. 10 is of order h and has been variously explained in terms of shot noise, zero point Johnson noise, and as a manifestation of the uncertainty principle. Most recently Koch, Van Harlinger, and Clarke[23] and Voss[24] have contributed to an understanding of this term. From a practical standpoint the intrinsic energy sensitivity can be expressed as

$$\varepsilon_w = \gamma_1 h\left(\frac{k_BT}{eI_oR}\right) + \gamma_2 h, \qquad (11)$$

where γ_2 is a numerical constant of order unity.

Equation 11 is a very powerful equation both from the point of view of SQUID design and from the point of view of interpreting SQUID performance. If one has the current-voltage characteristics of a SQUID for various values of applied flux and if the critical current modulation depth is of order 50%, then the expected noise performance is very simply given by Eq. 11 where I_oR can be deduced directly as indicated in Fig. 2. At 4.2K $k_BT/e \approx$ 360μV. Thus to achieve $\varepsilon \approx$ a few h one requires an I_oR product of a few hundred μV. It is important to realize that Eq. 11 holds for any $\beta_c \lesssim 1$. To enhance SQUID performance one must attempt to make I_oR as large as possible (keeping $\beta_c < 1$) while simultaneously keeping $\beta \approx 1$. From Eq. 1 we have

$$I_oR = \left(\frac{\beta_o j_j \phi_o}{2\pi c}\right)^{1/2}, \qquad (12)$$

where j_1 is the critical current density of the junctions and c is the junction capacitance per unit area. For a given technology c is fixed, and thus j_1 becomes the key to achieving a low value of ε_w. The condition that $\beta = 1$ implies that

$$2j_1AL = \phi_o \text{ ,or } AL = \frac{\phi_o}{2j_1}, \qquad (13)$$

where A is the junction area. Small values of ε_w thus require high j_1 and correspondingly low values of AL. If one's goal is to produce a low value of ε_w without regard to coupling, then it may be convenient not to use the smallest possible A, but rather to lower L to satisfy Eq. 13. This may well be the case if one desires to keep parasitic capacitance small compared with junction capacitance. If, on the other hand, one desires to couple to the SQUID then a higher L with very small junction areas (assuming parasitics can be kept low) is desirable.

The theory discussed above has in general been in good agreement with experimental results, although the exact values of γ_1 and γ_2 are still somewhat in question. Unfortunately white noise is not the only noise intrinsic to dc SQUIDs. 1/f noise is also present, and historically it has been considerably higher than what can be accounted for by known mechanisms.[17] There are numerous low frequency applications where a knowledge of 1/f noise in the SQUID is imperative. Recently, Ketchen and Tsuei[25] have used the thermal fluctuation theory for 1/f noise in in tunnel junctions originally developed by Clarke and Hawkins[26] to explain the 1/f noise in a small-area tunnel junction dc SQUID. This theory for SQUID 1/f noise will be briefly reviewed here, again with an emphasis on the importance of the I_oR product.

According to the thermal fluctuation model the junction volume (the region within a Ginzburg-Landau coherence length of the tunnel barrier) will undergo thermal fluctuations given by $(\Delta T)^2 = k_BT^2/C_v$ where C_v is the heat capacity of the junction volume. These fluctuations will have a power spectrum S_T which must obey the normalization condition

$$\int_0^\infty S_T(f)df = k_BT^2/C_v. \qquad (14)$$

If one assumes that $S_T(f) \propto 1/f$, independent of frequency, the normalization cannot be met. Voss and Clarke[27] have suggested that with a faster rolloff above some high frequency knee f_1 and a levelling off below some low frequency knee f_2, the normalization condition can be met, and $S_T(f)$ over a wide range will be given by

$$S_T(f) = \frac{k_BT^2}{GC_vf}, \qquad (15)$$

where it is assumed that $G \approx 2\pi$. (G depends logrithmically on f_1/f_2 and may possibly be larger or smaller by a factor of 2 or more.)

Fluctuations in temperature lead to fluctuations in I_o and consequently fluctuations in the flux in the SQUID. Let $C_v = \kappa C$. Assuming $\beta \approx \beta_c \approx 1$, it can be shown that[25]

$$\varepsilon_f \approx \frac{k_BT^2(I_oR)^2}{2\kappa f}\left(\frac{d\beta}{dT}\right)^2. \qquad (16)$$

This expression depends only on materials parameters and the I_oR product. Combining Eq. 11 and Eq. 16 and assuming for simplicity that $\gamma_1 = \gamma_2 = 1$ an expression results for the total intrinsic energy sensitivity (white plus 1/f):

$$\varepsilon \approx \frac{hk_BT}{eI_oR}\left\{1 + \frac{f_o}{f}\right\} + h \qquad (17)$$

where f_o is given by

$$f_o \approx \frac{T(I_oR)^3}{4\kappa\phi_o}\left(\frac{d\beta}{dT}\right)^2 \qquad (18)$$

While the intrinsic energy sensitivity in the white noise region, ε_w, decreases as $(I_oR)^{-1}$, the 1/f noise component of the energy sensitivity, ε_f, is predicted to increase as $(I_oR)^2$. The crossover frequency between ε_f and ε_w thus increases as a rate of $(I_oR)^3$.

As the temperature is lowered the 1/f noise in a tunnel junction dc SQUID should decrease, eventually going as $(1/T)(d\beta/dT)^2$ as $T \to 0$. While one might expect a significant reduction in the 1/f noise as T is decreased from 4.2K to, say, 2K the actual change will depend on the detailed temperature dependencies of κ and β. Clarke and Hawkins[26] generally found only small variations in the noise of their single junction samples over the temperature range of 1.5K to 4.2K.

As an example consider the cylindrical tunnel junction dc SQUID reported by Clarke, Goubau and Ketchen[17] which had junction areas of $\sim 10^4\mu m^2$. For this SQUID $I_oR \approx 1\mu V$, $\kappa \approx 6 \times 10^{-3} JK^{-1}F^{-1}$, and $d\beta/dT \approx 0.3K^{-1}$. Inserting these values into Eq. 16 one predicts $\varepsilon_f \approx 3h$ (1 Hz/f). The measured value was a factor of 100 greater. It is not altogether clear whether the excess 1/f noise was intrinsic to the SQUID or somehow an artifact of the readout circuitry. Equation 16 does fairly accurately predict the low frequency noise measured by Ketchen and Tsuei[25] in a small-area tunnel junction SQUID, (junction areas $\sim 10\mu m^2$) where the noise unambiguously originated in the SQUID. At present there is no other data in the literature on 1/f noise in SQUIDs of low ε_w. Measurements of white noise on such SQUIDs have been made with $f > f_o$ so that the validity of Eq. 16 has neither been confirmed nor disproved in these cases.

Readout Schemes

The noise sources discussed in the previous section are intrinsic to the dc SQUID. In order to use a SQUID to measure changes in flux it is necessary to read out the SQUID with some form of low temperature and/or room temperature electronics. If one is to take advantage of the extreme sensitivity of the SQUID it is highly desirable that the noise of the SQUID plus its readout system be dominated by the intrinsic noise of the SQUID. The traditional circuit developed by Clarke et. al.[17] to read out the dc SQUID is

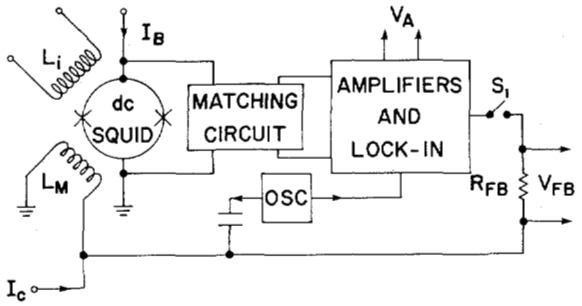

Fig. 4 Conventional phase locked loop dc SQUID readout scheme. With S_1 open this system can also be used to read out the dc SQUID in a small signal amplifier mode in the range of 10-100 kHz.

shown in Fig. 4. The SQUID is biased in the voltage state with some constant current I_B. A helium temperature impedance matching circuit consisting of either an LC circuit or a resonant transformer[28] is interposed between the SQUID and the low noise room temperature FET preamplifier. This circuit, which typically has a resonant frequency of 100 kHz, steps up the relatively low SQUID resistance ($\sim$ 1 Ω) to the $\sim$ 20 kΩ required for optimum FET noise performance. The SQUID is driven by a sinusoidal modulation flux of amplitude $\sim \phi_o/4$ generated via a current through the modulation coil L_M. The amplitude of the 100 kHz signal at the output of the matching circuit is periodic in the quasistatic flux in the SQUID. This signal is amplified first by the FET preamplifier and then by a subsequent tuned amplifier. The amplified 100 kHz signal is lock-in detected integrated and, with switch S_1 closed, fed back as a current via the feedback resistor, R_{FB}, to the modulation coil to cancel any charge in applied flux. The voltage appearing across the feedback resistor, V_{FB}, is thus proportional to the flux applied to the SQUID.

This readout system, dominated by intrinsic SQUID noise at least above $\sim 10^{-2}$ Hz, has proved to be extremely versatile and has been used extensively with dc SQUIDs having $I_oR \sim 1\ \mu V$ and $\varepsilon_w \sim 4x10^3h$. With the resonant transformer readout scheme a 3 db rolloff frequency of $\sim$ 40 kHz and a flux slewing rate of several times $10^5\ \phi_o\ s^{-1}$ at 1 kHz have been achieved along with a dynamic range on the order of 10^7. This design has the valuable feature that at least for a perfectly symmetric SQUID the output is independent of small changes in I_B or symmetric changes in the I_o's of the junctions such as might be introduced by drifts in bath temperature. It is also insensitive to drifts in amplifier gains. An excellent discussion of the details of operation of this type of readout circuitry is given in a recent review article by Giffard.[29]

The success of this readout system derives in part from the fact that the current-voltage characteristic of a SQUID with $I_oR \approx 1\mu V$ is very noise rounded and the $V(\phi)$ characteristic is smoothly varying - approximately sinusoidal in form. In the ac modulation technique the flux noise of the system is effectively the average over the flux bias points swept out by the modulation. The SQUID spends most of its time in regions of comparatively high $\partial V/\partial\phi$ so the noise is not seriously degraded from what it would be if the SQUID were always flux biased at points of maximum $\partial V/\partial\phi$. It has been suggested that a square wave flux modulation be used to improve the situation somewhat and perhaps to realize an improvement by a modest factor ($\lesssim$ 2X) in S_ϕ.

The new generation of low ε_w SQUIDs to be discussed in the next section cannot be effectively read out with the readout scheme just described. The problem is that for these SQUIDs the noise rounding is very small. The $V(\phi)$ characteristics exhibit sharp structure, and regions of high $\partial V/\partial\phi$ and low noise are frequently only a small fraction of a flux quantum in width (i.e., $\sim 10^{-2}\phi_o$). Thus for a sinusoidal flux modulation most of the time is spent in regions of low sensitivity and overall performance is poor. In principle, square wave flux modulation can get around this problem, although in practice no one has reported doing this. Instead, many of these recent low noise SQUIDs have been read out in a small signal amplifier mode. The most widely used circuit has been essentially the one shown in Fig. 4 with the switch S_1 open. A very small amplitude ($\Delta\phi \approx 10^{-4}\phi_o$) ac modulation flux at the matching circuit resonant frequency is applied to the SQUID via a current through L_M. The quasistatic flux bias position can be adjusted by changing the dc current I_c. One then measures the amplitude of the output voltage across the FET preamp, V_A, and divides this quantity by $\Delta\phi$ to get $\partial V/\partial\phi$. The oscillator is turned off and the noise voltage per $Hz^{1/2}$ is then measured at the preamp output, at the matching circuit resonant frequency, and in a bandwidth narrow compared with the bandpass of the matching circuit. The ratio of these two measurements gives $\sqrt{S_\phi}$. Voss has automated such a readout system so that one can relatively rapidly evaluate SQUID performance over a wide range of ϕ and I_B to find the optimum operating point.[30] This has proved to be a very useful technique for evaluating the high frequency (f > 10kHz) white noise performance of ultra low noise dc SQUIDs at specific frequencies.

For f $\lesssim$ 10kHz the technique discussed above begins to have problems because of the dominance of the low frequency noise of the FET. Ultimately, one is extremely interested in the noise performance of dc SQUIDs in the dc to a few kHz range. A scheme successfully used to make measurements in this frequency range makes use of an S.H.E. rf SQUID as a low noise preamplifier to read out the dc SQUID.[25] A circuit diagram of this scheme is shown in Fig. 5. A small change ($\Delta\phi = 10^{-4}.\phi_o$) in the quasistatic flux applied to the SQUID is introduced by making a calibrated change in I_c. The change in the room temperature output voltage of the rf SQUID phase locked loop is measured and divided by $\Delta\phi$ to get $\partial V/\partial\phi$. The noise power spectrum of the output voltage of the phase locked loop is then measured. This spectrum divided by $\partial V/\partial\phi$ gives S_ϕ for the dc SQUID. When properly configured the system is dominated by dc SQUID noise from dc out to a few kHz. The details of the matching circuits and filters and the value of the standard resistor R_{STD} depend strongly on the characteristics of the dc SQUID to be studied. Again one must explore over a wide range of applied flux and bias current I_B to find locations of optimum performance.

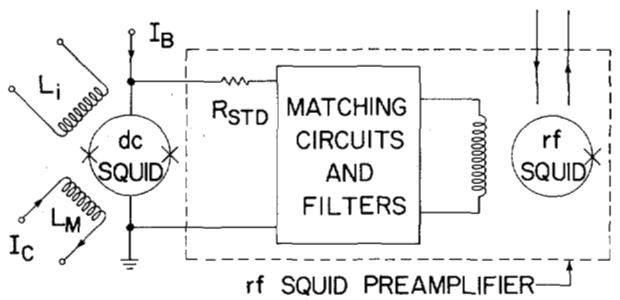

Fig. 5 rf SQUID preamplifier circuit used to read out the dc SQUID in a small signal amplifier mode in the range of dc to a few kHz.

These small-signal amplifier readout schemes, while providing valuable information on the noise performance of the latest generation of dc SQUIDs, by no means constitute a final solution to the readout problem. Although there exists a class of experiments which could be done reading out the SQUID in this fashion, by in large a proper phase locked loop readout scheme is desired. It is possible that an adaptation (such as square wave flux modulation) of the standard dc SQUID feedback system may be adequate. Further refinements of this system may be necessary or some more revolutionary approach may be in order.

The New Generation of dc SQUIDS

Throughout the mid and late 1970s the cylindrical dc SQUID designed by Clarke et. al.[17] at U.C. Berkeley proved to be the most successful dc SQUID. Noise performance somewhat better than that of commercially available rf SQUIDs together with well

developed coupling and readout schemes made this SQUID very useful for numerous applications. A detailed description of the Berkeley dc SQUID can be found in a number of other places[17,31,32] and will not be repeated here. Suffice it to say that even today this SQUID with $\varepsilon_w \approx 4000h$ and $\varepsilon_w^c \approx 10{,}000h$ remains a leader as far as dc SQUIDs suitable for general practical applications are concerned.

During the last two years, however, a new generation of ultra-low noise SQUIDs has appeared. These SQUIDs properly outfitted with useable input coils and flux-locked loop readout schemes should ultimately lead to practical SQUID systems orders of magnitude more sensitive than those of the 1970s. In this section an attempt will be made to review the status of this new generation by briefly describing some of its prominent members. For the most part work reported thus far has concentrated on producing SQUIDs with low values of ε_w.

The first big step downward on the intrinsic energy scale from the 4000h Berkeley cylindrical SQUID was taken by Hu, Jackel, Epworth and Fetter[33]. They fabricated a planar 200 pH SQUID using self shunting Pb-GeSn-Sn tunnel junctions with an I_oR product of about 300 μV. Using a phased locked loop readout scheme they measured an intrinsic energy sensitivity in the white noise region of 150h at 2K. This is considerably higher than one would expect from Eq. 10. It is possible that a careful small signal amplifier analysis of this SQUID would have revealed regions of considerably higher sensitivity. The 1/f noise was not reported.

Subsequently Koch, Van Harlingen, and Clarke[34] produced a 1 nH planar SQUID using 100 μm^2 Nb-NbOx-Pb tunnel junctions with AuCu shunts. With an I_oR product of $\sim$ 7 μV this SQUID read out in an FET-small signal amplifier configuration was found to have a minimum intrinsic energy sensitivity of about 300h, in reasonable agreement with Eq. 10. Again no 1/f noise performance was reported.

Another big step down the intrinsic energy sensitivity scale was taken by Ketchen and Voss[18] whose Pb alloy SQUID exhibited a minimum intrinsic energy sensitivity of 5h. This was a factor of 30 reduction over the best previous SQUID[33] and demonstrated for the first time the feasibility of operating a SQUID with ε_w on the order of h. This SQUID was fabricated using the Pb alloy process developed by IBM to produce Josephson logic circuits.[35] With a SQUID inductance of 11.5 pH, 10 μm^2 junctions, and $j_1 = 10^3$ Acm^{-2}, the planar, groundplaned SQUID had $I_oR \approx 200$ μV. Measured in the FET-small signal amplifier mode, the minimum intrinsic energy sensitivity was found to be 5h both at 4.2K and 1.7K. 5h is well within the range predicted by Eq. 11. The failure of ε_w to scale with temperature is not completely understood although it may be related to the proximity of the device to hysteresis. Subsequently the noise performance of this SQUID was studied in the range of frequencies from 0.5 Hz to 4 kHz by Ketchen and Tsuei[25] using an rf SQUID readout system as described in the previous section. The low frequency noise was found to be approximately 1/f in form. It crossed the white noise at about $f_o =$ 1 kHz, in good agreement with Eq. 18.

An all Nb planar SQUID having 1 μm^2 junctions shunted with PdSi shunts was produced by Voss, Laibowitz, Raider, and Clarke[36] This SQUID had a self inductance of about 1 nH and an I_oR product of about 50 μV. Using the FET-small signal amplifier readout scheme these workers found a minimum intrinsic energy sensitivity of 39h at 4.2K and 17h at 1.7K, and good agreement with Eq. 10.. The all Nb fabrication is obviously a strong feature of this SQUID from the point of view of mechanical integrity. No information on the 1/f noise performance of this SQUID is available.

The most sensitive SQUID in the literature at the time of this writing is one that makes use of nanostripes, the fabrication of which was pioneered by Laibowitz, Broers, Yeh, and Viggiano.[37] Voss, Laibowitz and Broers[38] have evaluated this 100 pH planar SQUID and measured a minimum intrinsic energy sensitivity at 4.2K of 3h. At lower temperatures the device became hysteretic. An extremely interesting feature of this SQUID is that the entire inductive loop including the two nanostripes is only about 1 μm^2 in size. The geometrical inductance is much less than the 100 pH SQUID inductance determined from the critical current modulation depth. The inductance of this SQUID is apparently dominated the "kinetic inductance" associated with the flow of electrons in the nanostripes which have cross sectional dimensions much less than the London penetration depth. The 1/f noise performance of this SQUID has not as yet been evaluated.

Finally, V. J. de Waal[39] has recently reported a Nb SQUID with 0.1 μm^2 tunnel junctions having $I_oR \approx 250$ μV. This SQUID with an inductance of about 1 nH as been operated in a flux locked loop as discussed in the previous section. The best intrinsic energy sensitivity measured thus far is about 150h. However, a big improvement will likely result if a small signal amplifier readout is tried. The 1/f noise performance of this SQUID has not yet been reported.

There are a number of other SQUIDs in the literature whose I-V characteristics or $V(\phi)$ characteristics are suggestive of very good low noise performance. In some of these cases no noise measurements are reported, while in others where measurements have been made, the technique used and results obtained indicate a strong possibility that the measurement was not intrinsic SQUID noise dominated. There is also new work discussed in these proceedings which may very well involve values of ε_w lower than any discussed here.[30,40]

Coupling

Most useful dc SQUIDs, as well as rf SQUIDs, have been inherently 3-dimensional objects, cylinders and toroids being the preferred geometries. Such structures have been relatively straightforward to fabricate while at the same time allowing fairly tight coupling between the SQUID and an input coil of useable self inductance. For these systems, with L_i in the range of a few hundred nH to a few μH, one generally can achieve $0.4 \lesssim k^2 \lesssim 0.8$ with 0.5 a typical value. The details of the design and fabrication of such traditional SQUIDs have been reviewed elsewhere[31] and will not be covered here.

The members of the recent generation of ultra-low noise dc SQUIDs, designed to demonstrate intrinsic energy sensitivity approaching Planck's constant, were all fabricated by means of techniques developed for planar substrates. Until very recently none of these SQUIDs were effectively coupled to. While low values of intrinsic energy sensitivity are of extreme interest from a scientific point of view, efficient means of coupling to these SQUIDs must be developed if the devices are ever to be of extensive practical use. There appear to be two possible strategies for resolving this problem. First one could incorporate the present small-area junction section of a new generation SQUID into a 3-dimensional structure to form a traditional toroidal or cylindrical SQUID. An example of the adaptation of the Berkeley all thin-film cylindrical SQUID to a 300 pH design with a wire wound input coil is discussed elsewhere[32]. Although such SQUIDs of lower self inductance may be possible, 300 pH is probably a reasonable lower limit on L that still allows tight coupling with a wire wound input coil. While a lower value of L is desirable from a noise standpoint, 300 pH would be acceptable. Unfortunately, no one seems to have a process for reproducibly fabricating small area junctions on a cylindrical surface. Even with such a process, SQUID production would most likely proceed - as in the past- on a one-at-a-time basis with each SQUID being treated as an individual throughout the fabrication process.

The second alternative to the coupling problem is to abandon the notion of traditional 3-dimensional coupling schemes altogether and to develop new coupling schemes that make use of the same high technology that enables one to fabricate small area tunnel junctions. A technique for tight inductive coupling between planar thin-film structures was originally proposed by Garwin in 1965.[41] This technique has been developed and experimentally verified by Arnett and Herrell[42,43] who make use of planar thin-film transformers in their design for the ac power distribution in Josephson logic systems. The first SQUID to make use of such a scheme was reported in an underpublicized paper by Dettmann, Richter, Albrecht and Zahn[44], who used a groundplaned fractional turn

SQUID with a 15-turn input coil to achieve $k^2 \approx 0.8$. A Pb-alloy process developed at IBM to fabricate Josephson logic devices[35], is now being used at IBM to fabricate planar SQUIDs with closely coupled planar input coils of up to 100-turns[45]. Work on fractional turn SQUIDs with input coils using a similar Pb-alloy process is in progress at NBS.[40]

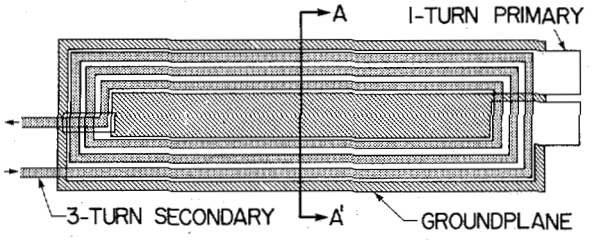

Fig. 6 Planar thin-film transformer.

Since the topic of tight, planar, inductive coupling is one which is relatively new to the SQUID community and one which will undoubtedly have a big impact on future SQUID design work, a section of this paper will be devoted to a discussion of an example that illustrates the basic principles involved. This example was chosen not to promote a particular SQUID design, but rather to illustrate the fundamental concepts of planar coupling and to demonstrate some of the relationships that will hold for any tightly coupled planar SQUID design. The structure to be considered is the transformer shown in Figs. 6 and 7. Assuming that the transformer is sufficiently long that end effects can be neglected, one can discuss the problem in terms of the cross section AA' shown in Fig. 7. The transformer has a wide 1-turn primary corresponding to a *SQUID inductance L, and a planar, n-turn spiral secondary* coil wound on top with inductance L_i and spacing s between this input coil and the primary. The linewidth of the input coil windings is a, with a pitch (center to center separation) of 2a. The windings are symmetrically located over the primary which has a width b = 2na. The separation between the inside edges of the primary is c. There is, in addition, a groundplane located a distance d below the primary. For simplicity it is assumed that all metal layers are of 3000Å thick superconducting Nb with a London penetration depth $\lambda = 860$Å. The quantities of interest in this example will be the inductance per unit length $\mathscr{L}$ of the transformer primary, the inductance per unit length $\mathscr{L}_i$ of the input coil, the mutual inductance per unit length $\mathscr{M}$ between the input coil and the primary, and the coupling constant $k^2 = \mathscr{M}^2 / \mathscr{L}_i\mathscr{L}$. The behavior of these quantities as a function of the distance d between the groundplane and the primary will be investigated. There are two special cases that are easily amenable to approximate analytical calculation. One of these has s << a and d << b; the other has s << a and $d = \infty$. These special cases will be discussed first, followed by numerical calculations for intermediate values of d.

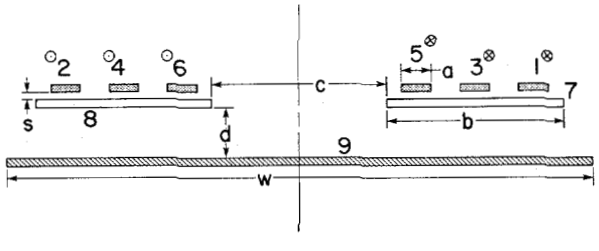

Fig. 7 Cross section AA' of the planar thin-film transformer. Conductors 1-6 consititute the secondary, or input coil. Conductors 7 and 8 are the primary, and conductor 9 is the groundplane.

In the first special case, s << a and d << b, one can make use of standard well known stripline formulas[46] to calculate the relevant quantities. In 0^{th} order, neglecting all fringe factors but including penetration depths, one has:

$$\mathscr{L} = 2\mu_o\left(\frac{d+2\lambda}{b}\right) \tag{19}$$

$$\mathscr{M} = 2n\mu_o\left(\frac{d+2\lambda}{b}\right) = n\mathscr{L} \tag{20}$$

$$\mathscr{L}_i = 2[n\mu_o\left(\frac{s+2\lambda}{a}\right) + n^2\mu_o\left(\frac{d+2\lambda}{w}\right)] = \mathscr{L}_s + n^2\mathscr{L} \tag{21}$$

The factor of 2 comes from the fact that there are two sides to the transformer. $\mathscr{L}$ is very simply the stripline inductance of a line of width b a distance d away from a groundplane where each conductor has a London penetration depth of λ. If the primary is open and a current i is sent through the input coil (see Fig. 7: in 1, out 2, in 3, out 4, etc.), there will be an image current i flowing on the top surface of the primary in a spiral pattern in the opposite sense immediately below the input coil. There will be a corresponding "sandbelting" current of (ni) uniformily distributed across the bottom side of the primary and flowing in the opposite direction of the top surface currents. A reverse image current of (ni) will in turn be induced in the groundplane. Thus a current of i in the input coil couples the same flux to the primary as a current of (ni) injected directly into the primary and $\mathscr{M} \approx n\mathscr{L}$. The self inductance of the input coil has two terms. The first, $\mathscr{L}_s$, is just the stripline inductance of the input coil with respect to the primary. The second term arises from the sandbelting current on the underside of the primary. On a given side of the transformer, each input coil term contributes i to this current and ($\mathscr{L}$i) to the flux between the groundplane and the secondary. This flux is coupled to all n turns of the input coil and adds $n\mathscr{L}$ to the input coil inductance. Since there are n turns each contributing i to the sandbelting current the total contribution to $\mathscr{L}_i$ is $n^2\mathscr{L}$.

For this case the coupling constant is given by

$$k^2 = \frac{\mathscr{M}^2}{\mathscr{L}_i\mathscr{L}} = \frac{d+2\lambda}{d+2s+6\lambda}, \tag{22}$$

where the fact that b = 2na has been used. It is noteworthy that b, a, and n have all dropped out, and k^2 depends only on d, s, and λ.

In the second special case, s << a and $d = \infty$ one can make use of standard stripline formulas together with existing solutions of the coplanar waveguide problem.[47]

$$\mathscr{L} = \mu_o\frac{K(m)}{K'(m)} \tag{23}$$

$$\mathscr{M} = n\mu_o\frac{K(m)}{K'(m)} = n\mathscr{L} \tag{24}$$

$$\mathscr{L}_i = 2n\mu_o\left(\frac{s+2\lambda}{a}\right) + n^2\mu_o\frac{K(m)}{K'(m)} = \mathscr{L}_s + n^2\mathscr{L} \tag{25}$$

In these expressions $m = (1+2b/c)^{-2}$, and K(m) and K'(m) are complete elliptic integrals of the first kind with argument the parameter m. The expression for $\mathscr{L}$ is the expression for the inductance per unit length of a coplanar waveguide consisting of zero thickness conductors of infinite conductivity. Provided the actual conductors are several London penetration depth thick and c >> λ, Eq. 23 will be very accurate. (Values of K(m) and K'(m) are tabulated in various books of tables, for example Ref. 48.)

The expression for $\mathscr{M}$ assumes that, as in the closely groundplaned case, the net effect - as far as flux coupled to the primary is concerned - of a current i in the secondary is the same as a current of (ni) inserted into the primary. The current flows on the underside of the secondary windings and is closely imaged by a reverse spiral current on the top surface of the primary. To balance this imaged spiral current on the primary a return current of magnitude

(ni) flows around the primary in the opposite sense with a spatial distribution identical to that which would exist if a current (ni) were applied directly to the primary.

As in the closely groundplaned case the expression for $\mathscr{L}_i$ consists of two terms, the first again being the stripline inductance of the secondary with respect to the primary. The second term $n^2\mathscr{L}$ is valid as before provided the return current flowing in the primary loop to balance the spiral image current couples as much flux to each secondary turn as it does to the primary. In the closely groundplaned case where the return current is a uniformly distributed sandbelt on the underside of the primary, it is obvious that the flux coupled to the primary will also be coupled to each secondary turn. In the absence of a groundplane, however, it is not so obvious that this is the case. The return current then flows on both the top and bottom surfaces of the primary with very pronounced peaking at the inside and outside edges of the primary. Nonetheless calculations (below) indicate that for physically reasonable dimensions very little flux leaks back around between the primary and secondary and Eq. 25 is a reasonable approximation.

In this case with no groundplane the coupling constant is given by

$$k^2 = [1 + \frac{2(s+2\lambda)K'(m)}{naK(m)}]^{-1} \qquad (26)$$

As n is increased (making b wider and keeping b/c constant), k^2 asymptotically approaches unity.

For comparison with Eqs. 19-26 and for results with intermediate values of d, the two-dimensional inductance calculation program developed by Chang[49] was used to numerically calculate $\mathscr{L}$, $\mathscr{M}$, $\mathscr{L}_i$ and k^2. Calculations were done for the transformer cross section shown in Fig. 7, with s = 0.2 μm, a = 5 μm, n = 3, b = c = 30 μm and w = 100 μm. The results of these calculations are shown in Fig. 8. $\mathscr{M}/n$ and $\mathscr{L}$ are shown as a single curve, although $\mathscr{M}/n$ is typically smaller by ~ 1%. A comparison between the results shown in Fig. 8 and the approximate analytical calculations is given in Table 1. The differences are due largely to

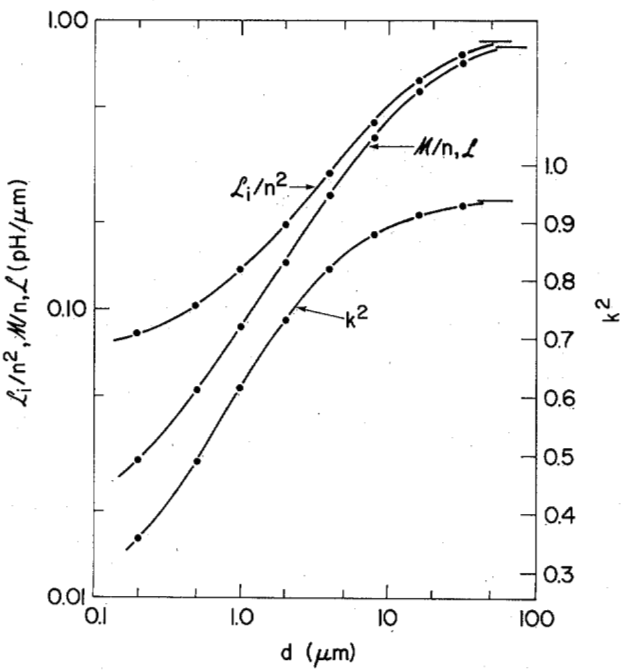

Fig. 8 Numerically calculated inductances and coupling constant for the thin-film transformer as a function of the distance from the underside of the primary to the top surface of the groundplane. The horizontal bars at the upper ends of the curves indicate the d = ∞ values.

	d = 0.2μm		d = 2μm		d = ∞	
	Eqs.	Fig. 8	Eqs.	Fig. 8	Eqs.	Fig. 8
$\mathscr{L},\mathscr{M}/n$	0.031	0.030	0.18	0.15	0.80	0.80
$\mathscr{L}_i/n^2$	0.093	0.083	0.24	0.20	0.86	0.84
k^2	0.33	0.35	0.74	0.73	0.93	0.94

Table 1: Inductance and coupling constants taken from numerical calculations (Fig. 8) compared with results from approximate analytical calculations (Eqs. 19-26).

the omission of fringe correction factors[50] from the simple stripline formulas.

Very good values of k^2 can be achieved with planar thin-film structures, even if a groundplane is used. Although the cases considered here are special in the sense that 2-dimensional calculations are adequate, it is clear that the basic conclusion demonstrated should hold in general provided the current through the input coil is closely imaged in the primary. Thus for a full turn SQUID in which any additional parasitic inductances are negligible the following equations should hold:

$$L = f(geometry) \qquad (27)$$

$$M = nL \qquad (28)$$

$$L_i = L_s + n^2L \qquad (29)$$

$$k^2 = [1 + L_s/n^2L]^{-1} \qquad (30)$$

The corresponding equations for a fractional turn SQUID[51] where each of m parallel loops has an inductance of L_l are:

$$L = \frac{L_l}{m} \qquad (31)$$

$$M = nL_l \qquad (32)$$

$$L_i = mn^2L_l + L_s \qquad (33)$$

$$k^2 = [1 + \frac{L_s}{mn^2L_l}]^{-1} \qquad (34)$$

The design of a planar SQUID with tight coupling thus reduces to finding a geometric shape for the SQUID inductance that gives the desired value of L while at the same time allowing for good imaging of the input coil current and low parasitic inductances getting into the junction structures. An interesting example of a fractional turn SQUID with a groundplane is given by Dettmann, Richter, Albrecht and Zahn.[44] A general solution for a full turn SQUID without a groundplane has been developed by Jaycox and Ketchen.[45] Work on coupled SQUIDs by Cromar and Carelli is presented in these proceedings.[40]

Conclusions

The I_oR product plays a crucial role in determining the noise performance of the dc SQUID. The thermal contribution to ε_w is ~ hk_BT/eI_oR which has a value of ~ h at 4.2K with I_oR = 360 μV. There is also a constant contribution to ε_w, attributable to shot noise and/or zero point fluctuations, that is equal to ~ h.

Several SQUIDs have now been demonstrated to have ϵ_w not far from this lower limit. The 1/f noise performance of the dc SQUID is predicted to degrade with increasing I_oR: $\epsilon_f \propto (I_oR)^2$. Existing experimental data agrees, but more data is needed. The performance of new dc SQUIDs with higher current density junctions $\left(I_oR \propto \sqrt{j_1}\right)$ and the performance of existing SQUIDs at much reduced temperature should be studied to better understand the ultimate limits of SQUID performance. Small signal amplifier readout schemes are presently in use to read out ultra-low-noise dc SQUIDs. A proper phase locked loop readout system that uses only a small region of the $V(\phi)$ characteristic is needed. Finally it appears that planar thin-film coupling schemes are the key to coupling to ultra low noise dc SQUIDs. Traditional 3-dimensional designs will likely give way to such schemes in the very near future.

Acknowledgement

The author acknowledges P. C. Arnett, W. H. Chang, D. J. Herrell, and J. M. Jaycox for helpful discussions on inductance.

References

1. R. C. Jaklevic, J. Lambe, A. H. Silver and J. E. Mercereau, Phys. Rev. Lett. 12, 159 (1964).
2. B. D. Josephson, Phys. Lett. 1, 251 (1962); Adv. Phys. 14, 419 (1965).
3. W. C. Stewart, Appl. Phys. Lett. 12, 277 (1968).
4. D. E. McCumber, J. Appl. Phys. 39, 3113 (1968).
5. J. E. Zimmerman and A. H. Silver, Phys. Rev. 141, 367 (1966).
6. J. Clarke and J. L. Paterson, Appl. Phys. Lett. 19, 469 (1971).
7. V. Radhakrishnan and V. L. Newhouse, J. Appl. Phys. 42, 129 (1971).
8. J. H. Claassen, J. Appl. Phys. 46, 2268 (1975).
9. J. Clarke, C. D. Tesche, and R. P. Giffard, J. Low Temp. Phys. 37, 405 (1979).
10. C. D. Tesche and J. Clarke, J. Low Temp. Phys., 29, 301 (1977).
11. C. D. Tesche and J. Clarke, J. Low Temp. Phys., 37, 397 (1979).
12. Y. H. Ivanchenco and L. A. Zil'berman, Zh. Eksperim. I. Teor. Fiz. 55, 2395 (1968) [Sov. Phys. JETP 28, 1272 (1969)].
13. V. Ambegaokar and B. I. Halperin, Phys. Rev. Lett. 22, 1364 (1969).
14. A. N. Vystavkin, V. N. Gubankov, L. S. Kuzmin, K. K. Likharev, V. V. Migulin and V. K. Semenov, Rev. Phys. Appl. 9, 79 (1974).
15. C. M. Falco, W. H. Parker, S. E. Trullinger, and P. K. Hansma, Phys. Rev. B10, 1865 (1974).
16. R. F. Voss, to be published in J. Low Temp. Phys.
17. J. Clarke, W. M. Goubau, and M. B. Ketchen, J. Low Temp. Phys., 25, 99 (1976).
18. M. B. Ketchen and R. F. Voss, Appl. Phys. Lett., 35, 812 (1979).
19. J. E. Zimmerman and D. B. Sullivan, Appl. Phys. Lett. 31, 360 (1977).
20. H. H. Zappe and B. S. Landman, J. Appl. Phys. 49, 344 (1978).
21. Y. Song and J. P. Hurrell, IEEE Trans. Magn., MAG-15, 428 (1979).
22. D. B. Tuckerman and J. H. Magerlein, Appl. Phys. Lett. 37, 241 (1980).
23. R. Koch, D. J. Van Harlinger, and J. Clarke, these proceedings.
24. R. F. Voss, to be published.
25. M. B. Ketchen and C. C. Tsuei, to be published in the proceedings of the 2nd International Conference on Superconducting Quantum Devices (held in W. Berlin, May 1980).
26. J. Clarke and G. A. Hawkins, IEEE Trans. Magn., MAG-11, 841 (1975).
27. Richard F. Voss and John Clarke, Phys. Rev. B., 13, 556 (1976).
28. M. B. Ketchen, W. M. Goubau, J. Clarke, and G. B. Donaldson, J. Appl. Phys. 49, 4111 (1978).
29. R. P. Giffard, to be published in the proceedings of the 2nd International Conference on Superconducting Quantum Devices (held in W. Berlin, May 1980).
30. R. F. Voss, R. B. Laibowitz, M. B. Ketchen, S. I. Raider, and A. N. Broers, to be published in the proceedings of the 2nd International Conference on Superconducting Quantum Devices (held in W. Berlin, May 1980); R. F. Voss, R. B. Laibowitz, A. N. Broers, S. I. Raider, C. Knoedler, and J. M. Viggiano, these proceedings.
31. J. Clarke, in Superconductor Applications: SQUIDs and Machines, B. B. Schwartz and S. Foner, Eds., New York: Plenum Publishing Corporation, 67 (1977).
32. M. B. Ketchen, J. Clarke, and W. M. Goubau, Future Trends in Superconducting Electronics, AIP Conference Proc. 44, New York (1978).
33. E. L. Hu, L. D. Jackel, R. W. Epworth, and L. A. Fetter, IEEE Trans. Magn., MAG-15, 585 (1979).
34. R. Koch, D. J. Van Harlingen, and J. Clarke (unpublished).
35. J. H. Greiner, C. J. Kircher, S. P. Klepner, S. K. Lahiri, A. J. Warnecke, S. Basavaiah, E. T. Yen, John M. Baker, P. R. Brosious, H.-C. W. Huang, M. Murakami, and I. Ames, IBM J. of R & D 24, No. 2 (1980).
36. R. F. Voss, R. B. Laibowitz, S. I. Raider, and J. Clarke, J. Appl. Phys. 51, 2306 (1980).
37. R. B. Laibowitz, A. N. Broers, J. T. C. Yeh, and J. M. Viggiano, Appl. Phys. Lett., 35 891 (1979).
38. R. F. Voss, R. B. Laibowitz, and A. N. Broers, to be published in Appl. Phys. Lett.
39. V. J. de Waal, to be published in the proceedings of the 2nd International Conference on Superconducting Quantum Devices (held in W. Berlin, May 1980).
40. M. W. Cromar and P. Carelli, these proceedings.
41. R. L. Garwin, U.S. Patent 3,184,674 (May 18, 1965).
42. P. C. Arnett and D. J. Herrell, IEEE Trans. Magn., MAG-15, 554 (1979).
43. P. C. Arnett, IEDM Tech. Dig., 485 (1979).
44. F. Dettmann, W. Richter, G. Albrecht and W. Zahn, Phys. Stat. Sol. (a) 51 K 185 (1979).
45. J. M. Jaycox and M. B. Ketchen, these proceedings.
46. J. C. Swihart, J. Appl. Phys., 32, 461 (1961).
47. C. P. Wen, IEEE Trans. Microwave Theory and Tech., MTT-17, 1087, (1969) and MTT-18, 318 (1970).
48. Handbook of Mathematical Functions, NBS Appl. Math Series 55, M. Abramowitz and I. A. Stegun, eds., U. S. Government Printing Office, Washington, D.C., 608 (1970).
49. W. H. Chang, these proceedings.
50. W. H. Chang, J. Appl. Phys., 50, 8129 (1979).
51. J. E. Zimmerman, J. Appl. Phys. 42, 4483 (1971).